

Study influence of forming process on microstructure and properties of deep hole thick wall pipe blank

LEI Bingwang^{1,a}, LIU Haijiang^{1,b*}, TU Mingjin^{1,c}, WANG Jiaoqi^{1,d}, WANG Xing^{1,e},
QIN Ruiting^{1,f}, KOU Yanyan^{1,g} and LIU Pengfei^{1,h}

¹Inner Mongolia North Heavy Industries Group Co., Ltd., Baotou, Inner Mongolia, P.R. China

^aleibingwang@163.com, ^b13848522181@163.com, ^ctumingjin2004@163.com,
^d13847284477@163.com, ^e13940565250@163.com, ^fbzyunzhonglang@163.com,
^g15354903902@163.com, ^hliupengfei@163.com

Keywords: Forming Process, Heavy Duty Extrusion, Radial Forging, Super High Strength and Toughness, Large Diameter Thick Wall Pipe Blank

Abstract. According to the demand for high strength and high toughness of deep hole thick wall pipe blank, basing on 36,000 tons of vertical extrusion machine, 3,000 tons of free forging press and 1,600 tons of radial forging machine. Using electroslag remelting to smelt Cr-Ni-Mo-V steel ingot as raw material, three forming processes were studied, including free forging and radial forging, solid extrusion and radial forging, and hollow extrusion and radial forging. The physical quantity distributions of stress, strain and strain rate in the deformation zone of billet blank in different forming processes were analyzed via numerical simulation technology. Combined with the numerical simulation results, three forming processes were carried out in engineering trial production. The trial production results show that the structure of the pipe blank produced by the hollow extrusion + radial forging process is uniform, the mechanical properties of the pipe blank at both ends of the sampling $R_{P0.2} \geq 1370$ MPa, $-40^\circ\text{CKV} \geq 28.0$ J, the mechanical properties of the full-length cross-section of the pipe blank $R_{P0.2} \geq 1381$ MPa, $-40^\circ\text{CKV} \geq 28.2$ J, the full-length yield strength is 28 MPa, and the comprehensive performance level is leading in the world.

Introduction

For a long time, people have actively explored new manufacturing methods (new processes, new equipment, etc.) of large forgings in order to economically obtain products with stable quality and excellent performance, and better serve aerospace, marine, national defense and other key areas of construction. As one of the most widely used weapons in various countries, barrel is the core component of artillery equipment and one of the important factors determining the performance and life of artillery [1-3]. The strength and toughness level of the barrel forgings have a decisive impact on the service life of the barrel, lightweight and the safety of the artillery [4-5]. With the rapid development of artillery to the path of large caliber, high bore pressure, high initial speed, long range and increasing muzzle energy, new requirements are put forward for the barrel. For the further improvement of the comprehensive performance of the barrel blank, such as strength and toughness, ablation resistance, integration of new generation of metallurgy, forming and heat treatment equipment, and further optimization of the manufacturing process to obtain ultra-high strength and toughness thick-walled billet, it is a major technical issue to support the development of future light large-caliber high bore pressure artillery and future high bore pressure main battle tank.

In order to improve the strength and toughness of thick-wall pipe blank for barrel, various countries have carried out in-depth research from the aspects of composition optimization [6-7], smelting process [8-9], forming process [8-9] and heat treatment process [10-11], and have achieved remarkable research results. Inner Mongolia North Heavy Industry Group Co., Ltd.

independently developed the world's largest ferrous metal vertical extrusion machine (Fig. 1) in July 2009, becoming the second enterprise in the world to master heavy extrusion technology. Continuously turning people's long-cherished wishes for heavy extrusion products into reality. Premium products such as extruding powder bar for large aircraft turbine disc, large caliber thick-wall seamless steel pipe of P91/P92 for thermal power, large caliber thick-wall seamless steel pipe of titanium alloy for marine construction, and TP316LN/TP316 series of large caliber pipes (rods) for fourth generation nuclear power have been mass produced, and the products performance are excellent. With our mature mastery of heavy extrusion technology, the integration of existing production equipment in our enterprise, developing "hollow extrusion + radial forging" composite forming process for medium alloy ultra-high strength and toughness barrel, and improving the ultra-high strength and toughness level of gun barrel, undoubtedly become a long-awaited technical research work in the field of artillery.

Based on 36,000 tons of heavy vertical extrusion machine, 3,000 tons of free forging and 1,600 tons of radial forging machine, this paper develops three kinds of composite forming process research on case1 "free forging + radial forging", case2 "solid extrusion + radial forging" and case3 "hollow extrusion + radial forging" for deep hole thick wall pipe billet, and makes beneficial exploration on the influence of forming process on the structure and performance of deep hole thick wall pipe billet.



Fig. 1. 36,000 tons heavy vertical extrusion production line.

Solid blanks and hollow blanks radial forging numerical simulation analysis

Radial forging machine with a unique high frequency pulse forging principle, realize short stroke, multi hammer, large tonnage, multi constraints of rapid forming, forging technology to bring a leap forward, but also for continuous research on metal forming process put forward new requirements. Using of deform11.0 simulation software (non MO module), for solid billet, hollow billet in the radial forging process of billet deformation area directly below the hammer strain, strain rate, stress field distribution and other physical quantities are analyzed by simulation technology. The rotary motion of manipulator and hammers movement synchronization, when hammers contact workpiece, the manipulator will stop rotating, feeding and other operations, four hammers began to hit the billet, when the hammer left the billet, the manipulator clamping billet rotating, feeding billet. The whole forging process of the manipulator, four hammers according to the above procedures cycle operation, until the end of the pass set task.

Numerical Simulation of solid blank radial forging process. Heads of the radial forging machine are distributed symmetrically along the circumference of 90°. The solid blank size of simulation

in this section is $\Phi 560 \times L$. After the first radial forging to $\Phi 490 \times L$ solid blank, the second radial forging to $\Phi 410 \times L$ solid blank, the first and second forging using the same hammer head. The length of the hammer head is 850 along the Z-axis direction of radial forging, and the hammer head is placed symmetrically about the XOY plane. Fig. 2 shows the CAD model of radial forging simulation for solid blank. The numerical simulation model of solid blank radial forging process assumes the following:

- (1) The elastic deformation of the material is ignored, and the material is regarded as rigid-plastic material;
- (2) The friction model is shear friction;
- (3) The hammer is regarded as a rigid body, and only heat exchange occurs between the hammer and the billet;
- (4) The temperature inside and outside the billet is uniform;

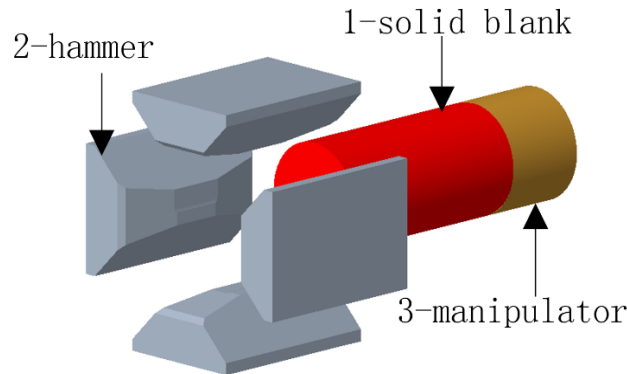


Fig. 2. Numerical simulation CAD model of four hammer head radial forging solid blank.

Initial temperature of solid blanks is 1230°C , initial temperature of hammer and other dies are 20°C , and the feeding speed of the billet is 30mm/s , and the frequency of the hammer is 3 times/s. Heat transfer coefficient between hammer and solid blanks is $1\text{ N}\cdot(\text{s}\cdot\text{mm}\cdot^{\circ}\text{C}^{-1})$, the shear friction coefficient is 0.2, and rotation angle of solid blanks between the two hammering is 13.5° . Solid blanks is clamped by manipulator to rotate and feed. The CAE simulation model of the solid bar with four hammers is established in software of Deform11.0, as shown in Fig. 3. During the first four-hammer radial forging deformation, solid blanks equivalent deformation of the axial section was "X"-shaped distribution, as shown in Fig. 4.

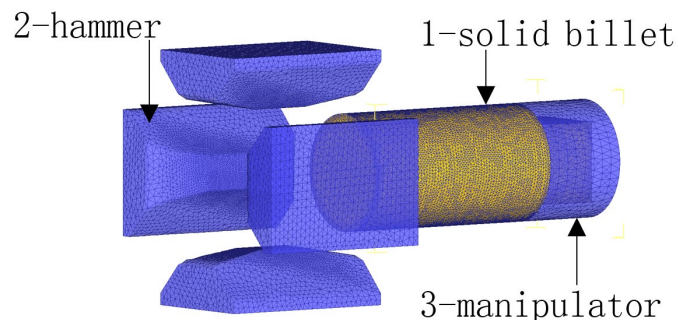


Fig. 3. Numerical simulation CAE model of four hammer radial forging solid blank.

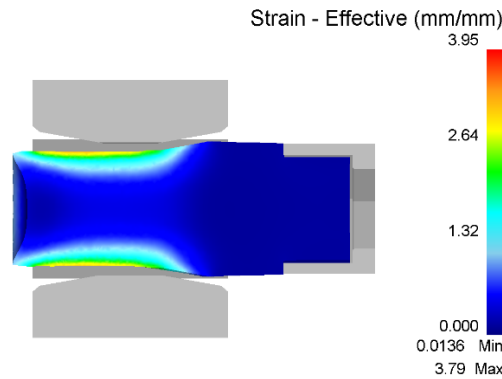


Fig. 4. Equivalent strain distribution of radial forging $\Phi 560 \times L$ solid blanks in axial section.

On the basis of the first pass precision forging deformation, the second pass radial forging is entered. The outer diameter of blank is radial forged from 490 mm to 410 mm. In the process of second pass radial forging, the distribution of stress, strain and strain rate at the transverse interface of large deformation of blank during the second radial forging process are shown in Fig. 5 and Fig. 6.

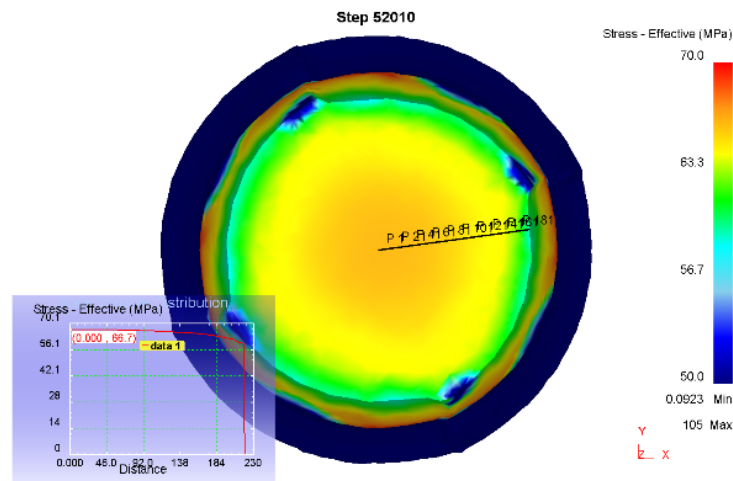


Fig. 5. Stress distribution of radial forging solid blank.

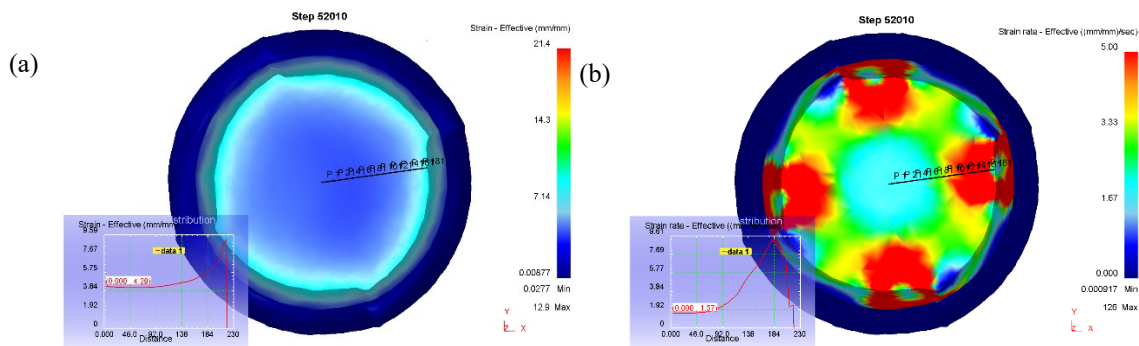


Fig. 6 (a) Strain and strain rate (b) Distribution of radial forging solid blank.

Numerical simulation of hollow pipe blank radial forging process. For hollow radial forging, four special hammer heads are used. Four hammer heads are distributed at 90° along the circumference and are the same relative to the hammer heads. The same hammer heads are used in the first and second passes. The specification of hollow pipe blank is $\Phi 560 \times \Phi 210 \times L$ in this section. The first pass is radial forged with $\Phi 150$ mm mandrel, and the hollow pipe blank specification is radial forged to $\Phi 490 \times \Phi 150 \times L$; second pass is radial forged with $\Phi 110$ mandrel, and the hollow pipe

blank specification is radial forged to $\Phi 410 \times \Phi 110 \times L$. Fig. 7 is the CAD model of the simulation of the precision forging of hollow pipe blank.

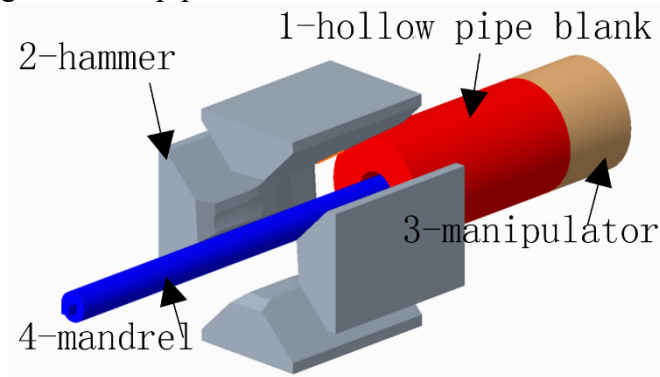


Fig. 7. Numerical simulation CAD model of four hammer head radial forging hollow pipe blank with mandrel.

The numerical simulation calculation model of hollow pipe blank radial forging process assumes:

(1) the elastic deformation of the material is ignored and the material is regarded as rigid-plastic material;

(2) the friction model is shear friction;

(3) the hammer and mandrel are regarded as rigid bodies, and only heat exchange occurs with the hollow pipe blank;

(4) the initial temperature hollow pipe blank t is uniform;

Initial temperature of hollow blank is 1230°C , initial temperature of hammer, mandrel and other molds are 20°C , manipulator holds hollow pipe blank to rotate and feed, rotation angle of hollow pipe blank between two hammers is 13.5° , the axial feeding speed is 30 mm/s , mandrel feeding speed is 0 mm/s , and precision forging machine hits 3 times/s . Heat transfer coefficient between hammer and hollow pipe blank is $1\text{ N}\cdot(\text{s}\cdot\text{mm}\cdot^{\circ}\text{C}^{-1})$, and heat transfer coefficient between extruded hollow pipe blank and mandrel is $0.4\text{ N}\cdot(\text{s}\cdot\text{mm}\cdot^{\circ}\text{C}^{-1})$. The CAE simulation model of hollow pipe blank for radial forging with four hammers in the software of *deform11.0* is shown in Fig. 8.

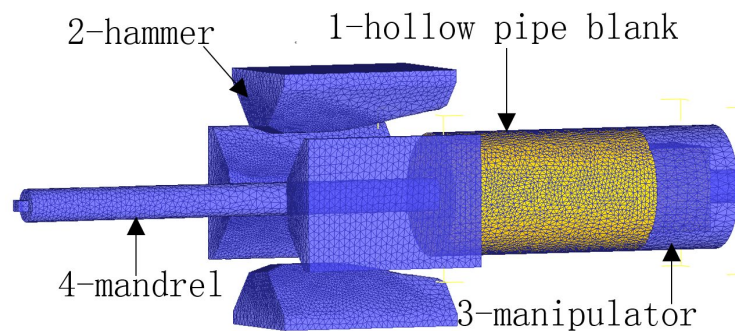


Fig. 8. Numerical simulation CAE model of four hammer head radial forging hollow pipe blank with mandrel.

In the radial forging process of $\Phi 560 \times \Phi 210 \times L$ hollow pipe blank with $\Phi 150\text{ mm}$ mandrel, the equivalent strain distribution of axial section of hollow pipe blank with mandrel in precision forging is shown in Fig. 9.

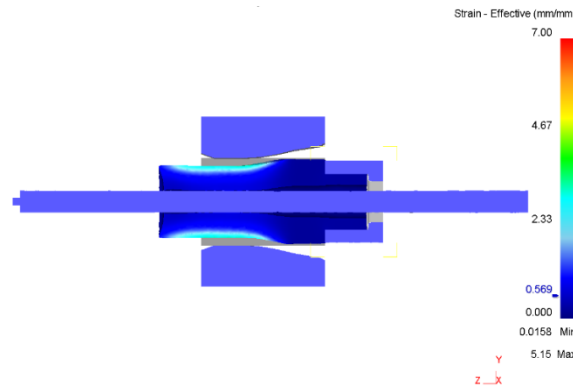


Fig. 9. Equivalent strain distribution of radial forging $\Phi 560 \times \Phi 210 \times L$ hollow pipe blank with mandrel in axial section.

Fig. 10 and Fig. 11 show the stress, strain and strain rate distribution in the deformation zone of $\Phi 490 \times \Phi 150 \times L$ hollow pipe blank radial forged to $\Phi 410 \times \Phi 110 \times L$ using $\Phi 110$ mandrel in the second pass.

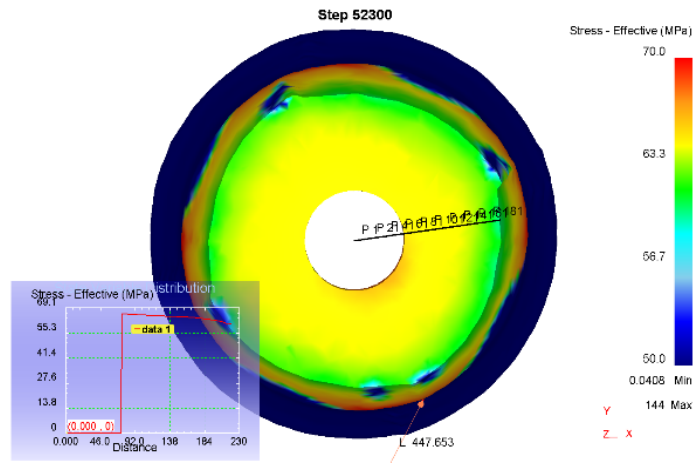


Fig. 10. Stress distribution of four hammer head radial forging hollow pipe blank with mandrel.

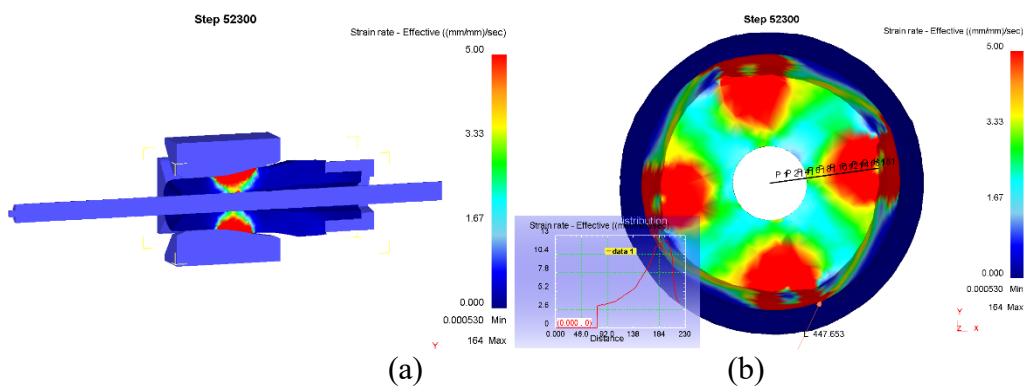


Fig. 11. Strain rate distribution of radial forging hollow pipe blank: (a) Axial section (b) Transverse section.

Comparison of deformation parameters of solid radial forging and hollow radial forging. As can be seen from the above numerical simulation, the radial forging method with two pairs of hammers can deform the workpiece around the workpiece during forging, ensuring the precise control of the size of the forgings. Four hammers are divided into two groups in the same plane for radial forging.

The billet is pressed in two directions. The wide plastic deformation is limited by the tool, and the plastic deformation of the metal is mainly axial extension.

In the process of solid blank radial forging, solid blank is formed by the unformed billet, which rotates at a certain rotation angle and is sent directly below the hammer, and is then formed under the action of four hammers. The solid blank to be formed in the middle stage of mandrel precision forging is rotated at a certain rotation angle and is sent directly below the hammer, and is deformed under the action of the compound angle hammer surface. The hollow pipe blank directly below the hammer of hollow radial precision forging is usually divided into three states of the pipe blank: "sinking area", "precision forging area" and "plastic area", and the metal is formed in different areas at the same time. In the "sinking area", the inner wall of the tube blank decreases the distance from the axis of the billet, and the thickness of the pipe wall remains basically unchanged. As pipe blank rotates and is sent, the inner hole of the tube blank contacts the mandrel, and at this time the tube blank is in the main deformation area, namely the "precision forging area". Fig. 12 shows the equivalent stress curve from inside to outside and along the radial direction on the transverse section of large deformation of blank during the instantaneous precision forging forming.

Fig. 12 shows the equivalent stress curve of the transverse section of blank with large deformation from inside to outside and along the radial direction during the transient radial forging of blank. The equivalent stress of solid billet at the corresponding position on the cross section along the radial direction 0mm~193 mm is slightly greater than that of hollow billet, the equivalent stress of solid blank and hollow blank at 193 mm away from the axis is equal to 62.5 MPa, and the equivalent stress of solid blank at 193mm away from the axis to the outer surface of the pipe is slightly less than that of hollow pipe blank. The equivalent stress of solid blank along the radial direction from the axis is distributed between 59.49 MPa ~66.73 MPa, and the equivalent stress gradually decreases from 66.73 MPa to 62.5 MPa along the radial direction from the axis, and the equivalent stress value is 62.5 MPa at 193mm away from the axis, and the equivalent stress decreases from 62.5 MPa to 59.49 MPa from 193 m along the radial direction to the outer surface; the equivalent stress of hollow billet with mandrel precision forging is distributed between 60.13 MPa ~65.78 MPa, and the equivalent stress gradually decreases from 65.78 MPa to 62.5 MPa along the radial direction from the nearest point to the axis, and the equivalent stress decreases from 62.5 MPa to 60.13 MPa from 193 mm along the radial direction to the outer surface.

Many scholars have found that with the increase of detection strain rate, the strength and toughness of the material are improved accordingly, and the sensitivity of strength improvement to strain rate is better than that of elongation [12-15]. For example, for the ultra-high strength hot-formed 30MnB5 automotive steel, in the low strain rate range (10^{-3} s^{-1} - 10^{-1} s^{-1}), the strain rate sensitivity of yield strength and tensile strength is low with the increase of strain rate; but in the high strain rate range (1 s^{-1} - 10^3 s^{-1}), the yield strength increases from 1520 MPa to 1620 MPa, an increase of 6.58%. However, there are few reports on the sensitivity of strain rate to high strength steel in the process of hot forming. In this paper, the quantitative simulation analysis is carried out for the change of strain rate of material in the deformation area in the hot forming process of solid/hollow stepped blank, and then the influence of strain rate on the strength, impact toughness and other properties of the product in the process of hot forming is revealed.

Fig. 13 shows that at the moment of forming solid and hollow blanks, the strain rate on the transverse interface of the maximum deformation of the billet in the "precision forging zone" increases first and then decreases along the radial direction from the axis area to the outer near surface. The strain rate of solid precision forging blank along the radial direction is distributed between 1.56 s^{-1} and 9.1 s^{-1} , and the strain rate value increases continuously from 1.56 s^{-1} at the axis to 9.1 s^{-1} at 180 mm away from the axis; then the strain rate value along the radial direction decreases continuously to 2.39 s^{-1} ; the strain rate value of hollow radial forging blank with mandrel along the radial direction is distributed between 3.10 s^{-1} and 12.38 s^{-1} , and the strain rate value

increases continuously from 3.10 s^{-1} near the mandrel surface to 12.38 s^{-1} at 193 mm away from the axis, and then decreases to 3.54 s^{-1} along the radial direction. It can be seen that in the process of four-hammer radial forging, the hollow radial forging blank with mandrel has a higher strain rate than the solid radial forging billet, which is more conducive to increasing the dislocation density of the metal in the thermal forming process, and provides a positive influence on improving the strength of the material.

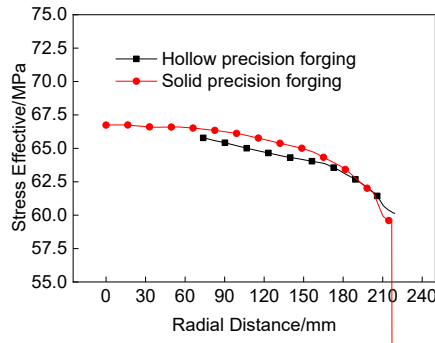


Fig. 12. Equivalent stress curve.

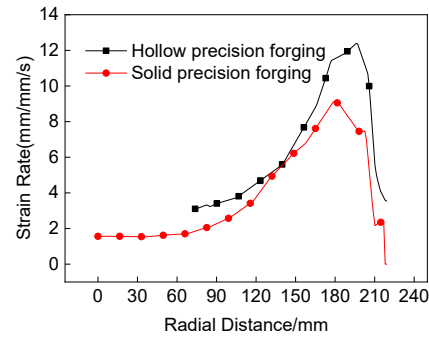


Fig. 13. Strain rate curve.

Numerical simulation analysis of moving force of mandrel in hollow radial forging. Considering the equipment capacity of 1600-ton four-hammer radial forging machine, the string force along the drawing direction is not more than $1 \times 10^5 \text{ N}$. Among the three combined forming schemes designed in this paper, there are problems in the radial forging process of four-hammer radial forging of hollow pipe blank with large aspect ratio and mandrel perforation. Therefore, four-hammer radial forging of hollow pipe blank with large aspect ratio is one of the key processes studied in this paper. In view of this problem, this paper carries out numerical simulation research. The CAD model established for numerical simulation analysis of four-hammer radial forging of hollow pipe blank with large aspect ratio is shown in Fig. 8. In Fig. 8, the specification of hollow radial forged pipe billet is $\Phi 560 \times \Phi 210 \times 1000$, and four hammer radial forging with large deformation is adopted. The length of hammer along the pulling direction of extrusion blank is 850 mm, and the maximum diameter of mandrel is 150 mm (taper 0.0016°) and the length is 1900 mm. The simulated reduction amount is used to radial forge the extrusion blank with outer diameter of 560 mm to $\Phi 390$ mm, and the single pass deformation reaches the large deformation model of 170 mm. The temperature of the simulated blank is 1230°C , the initial temperature of the hammer, mandrel and other dies is 20°C , the feeding speed of mandrel is 0 mm/s, the feeding speed of billet is 30 mm/s, and the frequency of radial forging machine is 3 times/s. The heat transfer coefficient between the extruded hollow pipe blank and the mandrel is 0.02, and the rotation angle is 13.5° . The friction coefficients between the inner surface of the extruded pipe blank and mandrel in the radial forging process were set as 0.3 and 0.05, and the force of mandrel when pulling and removing mandrel in the numerical simulation of the four hammer radial forging process is simulated.

Through simulation analysis, when the shear friction coefficient is 0.3, the mandrel needs 20 tons of force in the radial forging hollow pipe blank within 15 seconds after the start of four-hammer precision forging, which is much higher than the load of the radial forging machine. Moreover, with the increase of the feeding amount of the blank under the four-hammer, the maximum stringing force required by the mandrel in the blank reaches $8 \times 10^5 \text{ N}$. When the friction coefficient is reduced to 0.05, the whole billet is fed directly under the hammer, and the maximum stringing force of the mandrel is $9.5 \times 10^4 \text{ N}$. Therefore, to realize the radial forging forming of the hollow pipe blank with large deformation and mandrel by four-hammer, the friction coefficient at high temperature should be less than 0.05. The force required for pulling and removing the mandrel

with different friction coefficients between the mandrel and the hollow pipe blank is shown in Fig. 14.

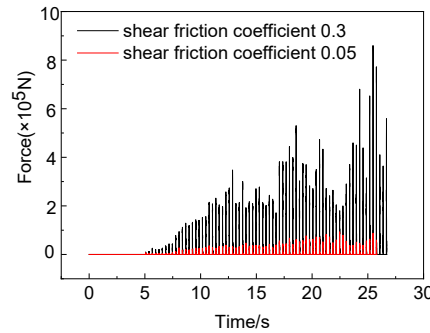


Fig. 14. Rod string pull-out load (friction coefficient 0.3, 0.05).

Trial-manufacture

Based on simulation results, three forming processes, including case1 "free forging + radial forging", case2 "solid extrusion + radial forging" and case3 "hollow extrusion + radial forging", were carried out. The electroslag remelted ingot of Cr-Ni-Mo-V medium and low carbon alloy was used in the trial-production.

Case 1 "free forging + radial forging"

Technical process of case1: 3000 tons of free forging blanking - radial forging solid blank - annealing - rough machining - quenching and tempering heat treatment - performance detection.

(1) Free forging solid blank

Using 3000 tons free forging press for three upsetting and three drawing blank. For the first upsetting, the electroslag ingot is heated to $1210^{\pm 10}^{\circ}\text{C}$, and the electroslag ingot is upset to 700 mm by ratio of 2.15. Then the FM forging method is used to draw the long ingot. The sum of the upper and lower forging amount in each pass is distributed between 25% and 28%. After forming side A of the ingot, the ingot to be formed is rotated 90° along the axis and then adjacent side B is forged. After multiple draws, the size is $600^{\pm 10} \times 650^{\pm 10} \times L$ blank. For the second upsetting, the billet was returned to the furnace and heated to $1210^{\pm 10}^{\circ}\text{C}$, and the blank was upset to 700mm. After multiple upsetting, the specification was $600^{\pm 10} \times 650^{\pm 10} \times L$. For the third upsetting, the billet was returned to the furnace and heated to $1210^{\pm 10}^{\circ}\text{C}$, and the blank was upset to 700mm. After multiple upsetting, the specification was $620^{\pm 10} \times 620^{\pm 10} \times L$. Then the upper and lower flat anvil chamfering, and then using the upper flat anvil, the lower V-shaped anvil forging into the size of $\Phi 620 \times L$ round rod.

(2) Radial forging solid stepped blank

The solid blank is freely forged, and then the blank is heated to $1150^{\pm 10}^{\circ}\text{C}$, and then radial forging is performed. The radial forging adopts R180 hammer head, blank feeding speed is 30mm/s, and radial forging frequency is 3 times/second. The solid billet of $\Phi 315 \times L$ is forged by multi-pass pressing. During last pass, stepped blank is finished, forging ratio between 2.72 ~ 5.58.

Case 2 "solid extrusion + radial forging"

Technical process of case 2: 15000t equipment upsetting blank - 36000t extrusion machine extruding solid blank - radial forging solid blank - annealing - rough machining - quenching heat treatment - performance detection.

(1) Extruding solid blank

The electroslag ingot is heated to $1260^{\pm 10}^{\circ}\text{C}$, the surface oxide skin is removed, and closed upsetting is completed on the 15000t equipment. The solid blank is heated to $1210^{\pm 10}^{\circ}\text{C}$, and 1100

series extrusion cylinder and $\Phi 535$ mm extrusion die are used on the 36000t extrusion machine to extrude $\Phi 525 \times L$ solid blank, with an extrusion ratio of 4.62. The extruded blank is heated to $1150^{\pm 10} \text{ }^\circ\text{C}$, and then radial forging is carried out. R180 hammer head is used for radial forging, with a billet feed rate of 30mm/s and a refined forging frequency of 3 times/second. The solid billet of $\Phi 315 \times L$ is forged by multi-pass pressing. During last pass, stepped blank is finished, forging ratio between 2.72 ~ 5.58.

Case 3 "hollow extrusion + radial forging"

Technical process of case3: upsetting and punching blank with 15000t equipment - 36000t extruding hollow pipe blank - radial forging hollow pipe blank - annealing - quenching heat treatment - performance detection.

(1) Extruding hollow pipe blank

The electroslag ingot is heated to $1260^{\pm 10} \text{ }^\circ\text{C}$, the surface oxide skin is removed, and the closed upsetting and punching blank are completed on the 15000t equipment. The hollow pipe blank is heated to $1210^{\pm 10} \text{ }^\circ\text{C}$, and 1100 series extrusion cylinder, $\Phi 535$ mm extrusion die, $\Phi 155$ mm extrusion mandrel are used on the 36000t extrusion equipment to extrude $\Phi 525 \times \Phi 155 \times L$ hollow pipe blank, with an extrusion ratio of 4.75.

(2) Radial forging solid stepped blank

The radial forging process of extruded blank is completed by passes. The first pass is pre-forging: the extruded billet is heated to $1200^{\pm 10} \text{ }^\circ\text{C}$, the inner hole is lubricated, and then the radial forging is carried out. R180 hammer head is used for radial forging, the billet feed rate is 30mm/s, and the precision forging frequency is 3 times/second. The extruded billet is radial forged into $\Phi 380 \times \Phi 110$, $\Phi 420 \times \Phi 110 \times L$ hollow stepped billet. The second pass is final forging: the pre-forged billet is heated to $1200^{\pm 10} \text{ }^\circ\text{C}$, and then the radial forging is carried out. R180 hammer head is used for radial forging, the blank feed rate is 30mm/s, and the radial forging frequency is 3 times/second. The pre-forged billet is radial forged into $\Phi 255 \times \Phi 60$, $\Phi 295 \times \Phi 60$, $\Phi 315 \times \Phi 60$ hollow stepped blank. The 2 solid stepped blanks trial-produced in case 1 and the 7 solid stepped blanks trial-produced in case 2 were machined into hollow stepped pipe blanks, and the same heat treatment process parameters were adopted to adjust the heat treatment of the 4 stepped hollow pipe blank trial-produced in case 3.

Performance testing

Test results of sampling at both ends of blank

A total of 13 stepped blanks were trial-produced in the three cases. Two stepped blanks were trial-produced in case1, serial numbered as 1~2., seven stepped blanks were trial-produced in case2, serial numbered as 3 ~ 9, and four pieces were trial-produced in case3, serial numbered as 10 ~ 13. Physical and chemical properties such as mechanical properties, microstructure and grain size were tested by sampling from both ends of each billet. Specific results are as follows:

(1) Mechanical property

The statistical results of mechanical properties of the 13 stepped blanks are shown in Table 1.

Table 1. Statistical results of mechanical properties of the 13 stepped blanks.

case	R _{p0.2} /MPa		Z%		-40°C AKV/J	
	range	average	range	average	range	average
1	1381~1354	1370.7	55~51	52.8	30.1~19.0	25.5
2	1380~1354	1363.7	61~54	56.6	33.1~25.1	28.6
3	1386~1370	1378.2	61~53	55.0	33.3~28.0	30.1

(2) Microstructure

The microstructure and grain size of 13 stepped blanks are shown in Table 2.

Table 2. Microstructure and grain size of stepped blanks.

No.	microstructure		grain size		
	end1	end2	end1	end2	
1	T.P.	T.P.	9	9	case1
2	T.P.	T.P.	9	9	
3	T.P.	T.P.	8	8	
4	T.P.	T.P.	9	9	case2
5	T.P.	T.P.	7	8	
6	T.P.	T.P.	9	9	
7	T.P.	T.P.	7	7	
8	T.P.	T.P.	9	9	
9	T.P.	T.P.	7	7	
10	T.P.	T.P.	8	8	case3
11	T.P.	T.P.	8	8	
12	T.P.	T.P.	8	8	
13	T.P.	T.P.	7	7.5	

Note: 1. “end1” expresses large diameter end of stepped blanks; “end2” expresses small diameter end of stepped blanks.

2. T.P. expresses Tempered Martensite Pearlite.

Full-length cross-sectional test results of stepped pipe blank

The section test of No. 12 hollow stepped pipe blank was selected, and there were 1 test pieces in each area at 200mm from the end face of large-diameter of the pipe blank, 1/4, 1/2, 3/4 from the full length of the end face of large-diameter, and 200mm from the end face of small-diameter, that is, 5 test pieces in total. There are two test samples for tensile, impact, (-40°C) and grain size on the same test piece, and the test samples for each type are numbered 1 ~ 10 from large-diameter end to small-diameter end.

Fig. 15 shows sectional test results of tensile test at room temperature. R_{p0.2}: 1381 MPa ~ 1409 MPa, yield strength difference 28 MPa, indicating that the strength uniformity of stepped pipe

blank reaches a relatively high level. Fig. 16 shows test results of low temperature impact toughness -40°C AKV : $28.2\text{ J} \sim 32.5\text{ J}$, indicating that the total length of hollow stepped pipe blank meets requirement of $-40^{\circ}\text{C AKV} \geq 25\text{ J}$.

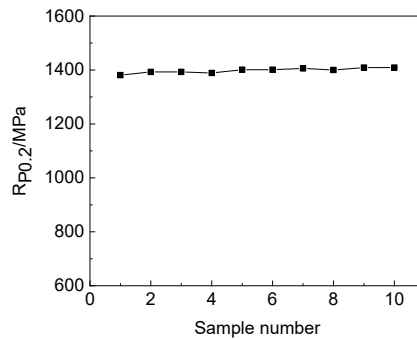


Fig. 15. Tensile strength and yield strength of cross sectional test.

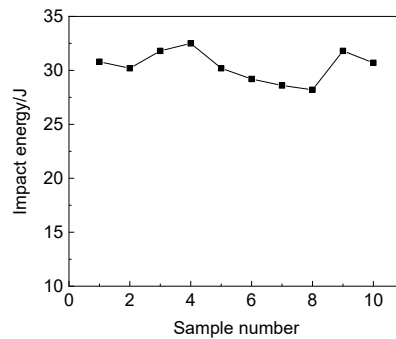


Fig. 16. Low temperature Impact toughness of cross sectional test.

Fig. 17 shows test results of cross-sectional grain size, and the grain size distribution ranges from $19.1\mu\text{m}$ to $23.5\mu\text{m}$.

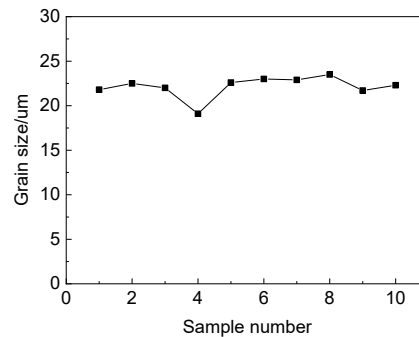


Fig. 17. Grain size.

Discussion

From the above physical and chemical test results, it can be seen that the mechanical properties of the stepped pipe blanks formed in case 2 "solid extrusion + radial forging" are significantly improved than those formed in case1 "free forging + radial forging". Using case1 "free forging + radial forging" process, the formed stepped blank $R_{p0.2}$: $1354\text{ MPa} \sim 1381\text{ MPa}$, -40°C AKV : $19\text{ J} \sim 30.1\text{ J}$, impact fluctuation value is 11.1 J . Using Case1 "free forging + radial forging", due to the use of upper and lower hammer heads and 3000 tons of free forging press blanks, the deformation degree and deformation temperature of ingot in each region are very different, and there are risks

such as large fluctuation value of mechanical properties difference and unstable performance. The lowest low temperature impact value of trial-produced blanks in this batch is 19 J and the fluctuation range is 11 J, that is, the fluctuation of -40°C AKV impact energy is 58.4%.

According to case 2 "solid extrusion blanking + four hammer head precision forging" process, the forming of 7 solid step billets is firstly closed upsetting and pressure maintaining in the 15,000 tons equipment of the 36,000 tons vertical extrusion production line. In the first stage of the deformation process of the ingot, three-dimensional compressive stress provides good conditions for the transformation of the organization of the ingot casting state to the organization of the plastic state, which is conducive to the uniformity of the subsequent products. In the subsequent extrusion forming process, the metal to be formed is extruded for the second time in the extrusion cylinder after three-dimensional compressive stress of 36,000 tons. Then solid blank is formed in the four-hammer radial forging under multi-directional constraints, which provides guarantee for the quality of blank. In this trial production of 7 to step billet $R_{p0.2}$:1354 MPa ~ 1380 MPa, -40°C AKV: 25.1 J ~ 31.1 J, and the impact fluctuation range is 8 J, that is, the low temperature impact energy fluctuation of -40°C AKV is reduced from 58.4% in case1 to 31.8% in case 2 "solid extrusion + radial forging".

Case 3 "hollow extrusion + radial forging" process was used to form 4 stepped hollow pipe blanks. First, the closed upsetting and pressure holding were used in the 15,000 tons equipment of 36,000 tons vertical extrusion line. During the deformation of ingot in the first stage, the three-way compressive stress was applied to provide good conditions for the transformation of the cast structure to the plastic structure of ingot. Then the through hole billet is made by perforating needle. During the perforating process, the metal of the ingot axis is greatly plastic deformed to further improve the internal and external consistency of the through hole billet. In the subsequent through hole billet extrusion forming process, the metal to be formed is extruded in the extrusion cylinder for the second time under the action of 36,000 tons of three-way compressive stress. Due to the action of the mandrel on the hollow blank, the distribution of metal flow velocity at the extrusion die is more uniform and consistent than that in case2. Then the billet is formed under the multi-direction constraint condition of four-hammer radial forging, which provides guarantee for the quality of the extrusion billet. In this paper, the mechanical properties of 4 stepped hollow stepped pipe blanks formed by hollow extruding and radial forging with four hammer heads and mandrel. $R_{p0.2}$:1370 MPa ~ 1386 MPa, -40°C AKV: From 28.0 J to 33.3 J, the impact fluctuation range is 5.3 J. On the basis of improving the yield strength, the impact fluctuation of -40°C AKV at low temperature decreased to 18.9%.

In addition, the sectional test of case 3 "hollow extrusion + radial forging" shows that the full-length performance of the stepped pipe blank meets the calculation requirements and the fluctuation range is small. Among them, $R_{p0.2}$:1381 MPa ~ 1409 MPa, difference 28 MPa, section shrinkage Z: 51% ~ 56%; -40°C AKV: 28.2 J ~ 32.5 J. In the tempering brittleness experiment, -40°C AKV: 28.3 J ~ 35.6 J.

Summary

Case 1 "free forging + radial forging", case2 "solid extrusion + radial forging" and case3 "hollow extrusion + radial forging" are three composite processes for manufacturing hollow pipe blank. The test results of yield strength are 1354 MPa ~ 1381 MPa, 1354 MPa ~ 1380 MPa, 1370 MPa ~ 1386 MPa, and the low temperature impact fluctuation value of -40°C AKV was 58.4%, 31.8%, 18.9%, respectively. The impact power of "extrusion + radial forging" is higher and more stable than that of "free forging + radial forging".

Hollow extrusion stepped hollow pipe blank is dissected, where $R_{p0.2}$:1381 MPa ~ 1409 MPa, section shrinkage Z: 51% ~ 56%; -40°C AKV: 28.2 J ~ 32.5 J, the tempering brittleness experiment

-40°C AKV: 28.3 J ~ 35.6 J, the results show that the full-length performance of hollow pipe blank meets technology requirements and the fluctuation range is small.

The solid blank $\Phi 490 \times L$ was radial forged to $\Phi 410 \times L$ with four hammer heads, and the hollow pipe blank $\Phi 490 \times \Phi 150 \times L$ was radial forged to $\Phi 410 \times \Phi 110 \times L$ with $\Phi 110$ mandrel. The strain rate on the transverse interface of blank in the two deformation processes was analyzed. The strain rates of solid radial forging blank ranged from 1.56 s^{-1} - 9.1 s^{-1} along the radial direction, and those of hollow radial forging billets with mandrel ranged from 3.10 s^{-1} to 12.38 s^{-1} along the radial direction. Compared with solid radial forging blanks, hollow radial forging blanks with mandrel had higher strain rates and better comprehensive mechanical properties.

A four hammer radial forging CAE model with mandrel for pipe blank with outer diameter of 560 mm, inner hole of 210 mm, and length of 1000 mm was established in the simulation software of Deform-3D. For the calculation of 0.05 and 0.3 different shear friction coefficients between mandrel and hollow blank, the simulation results show that when the friction coefficient between mandrel surface and hollow blank deformation zone is controlled less than 0.05 in the radial forging process, the large-scale pipe blank with mandrel can be radial forged.

References

- [1] Y.F. Xu, C.L. Shan, P.K. Liu, Review of the research on gun barrel life-span prolongation, *Journal of gun launch & control* (2019) 90-95. <https://doi.org/10.19323/j.issn.1673-6524.2019.04.019>
- [2] P.K. Liu, D. Yang, J. Wang, Study on ablation and wear properties of barrel materials, *Journal of gun launch & control* (2021) 28-33. <https://doi.org/10.19323/j.issn.1673-6524.2021.04.006>
- [3] M.L. Zhu, L.L. Liu, F.Z. Xuan, J. Effect of frequency on very high cycle fatigue behavior of a low strength Cr-Ni-Mo-V steel welded joint, *Int. J. Fatigue* (2015) 77-166. <https://doi.org/10.3901/JME.2016.12.023>
- [4] Y.Q. Ou, C.G. Yu, Y.C. Zhang, Development of erosion and wear of gun barrel, *Ordnance industry automation* (2012) 44-46. <https://doi.org/10.3969/j.issn.1006-1576.2012.06.014>
- [5] S.S. Zhang, Material process and service life of gun barrel, *Journal of xi'an institute of technology* (1989) 1-9. <https://doi.org/10.16185/j.jxatu.edu.cn.1989.01.001>
- [6] Y. Lv, J. Hu, Z.N. Ren, Process in steel used for large-calibre thick-wall gun barrel, *Ordnance material science and engineering* (2013) 142-146. <https://doi.org/10.14024/j.cnki.1004-244x.2013.02.011>
- [7] N. Zhang, C.R. Lv, L. Xu, Currents status and development trend of gun barrel steel, *J. China metallurgy* (2019) 6-9. <https://doi.org/10.13228/j.boyuan.issn1006-9356.20190160>
- [8] X.D. Yuan, L.Q. Gao, H.F. Zhang, Development and prospect of gun barrel materials, *Mater. Develop. Appl.* (2017) 98-104. <https://doi.org/10.19515/j.cnki.1003-1545.2017.05.019>
- [9] J.F. Huang, J. Zhang, J.Y. Chen, Failure mechanisms of gun barrels and the development of gun steel, *Journal of gun launch & control* (2023) 10-29. <https://doi.org/10.19323/j.issn.1673-6524.2023.01.002>
- [10] D.B. Sun, Z.L. Jin, W. Li, Effect of tempering process on microstructure transformation of large-caliber 40CrNiMoV, *Ordnance material science and engineering* (2023) 72-76. <https://doi.org/10.14024/j.cnki.1004-244x.20230516.004>

- [11] Y. Liu, M.Q. Wang, G.Q. Liu, Effects of tempering temperature on microstructure and mechanical properties of 40CrNiMoV steel, *Journal of gun launch & control* (2019) 90-95. <https://doi.org/10.13251/j.issn.0254-6051.2014.06.012>
- [12] J.T. Liang, C.Z. Zhao, H.X. Yin, Strain rate sensitivity of ultra-high strength hot stamping steel, *Chinese Journal of Engineering* (2018) 1083-1090. <https://doi.org/10.13374/j.issn2095-9389.2018.09.009>
- [13] H.J. Cai, J.F. Hu, R.B. Song, Plastic deformation microscopic mechanism of cold rolled dual phase steel DP1200 under high strain rate deformation, *J. Mech. Eng.* (2016) 23-29. <https://doi.org/10.3901/JME.2016.12.023>
- [14] W. Zhang, Y. Pan, H.S. Liu, Effect of strain rate on properties of dual phase steel with high formability, *Iron and steel* (2022) 123-127. <https://doi.org/10.13228/j.boyuan.issn0449-749x.20210619>
- [15] H.N. Liu, Y.D. Mei, L.B. Liu, Influence of strain rate on properties for low alloy high strength steel, *Forg. Stamp. Tech.* (2023) 253-257. <https://doi.org/10.13330/j.issn.1000-3940.2023.06.034>